

Chapter 2

Programmable Hybrid Integrated Circuit/Microfluidic Chips

Caspar Floryan, David Issadore, and Robert M. Westervelt

Abstract The miniaturization of laboratory functions onto microfluidic chips is leading a paradigm shift in biotechnology, analogous to the transformation of electronics by the integrated circuit (IC) 50 years ago. The microfabricated pipes, pumps, valves, and mixers of microfluidics enable small volumes of reagents, samples, and individual living cells to be controlled on low-cost, portable chips. However, a microfluidic chip that can be programmed to perform the wide range of chemical and biological tasks required for medical and scientific analysis, akin to a microprocessor in electronics, remains a challenge. Here, we review work done by our group to develop hybrid IC/microfluidic chips that can simultaneously control thousands of living cells and picoliter volumes of fluid, enabling a wide variety of chemical and biological tasks.

2.1 Introduction

Advances in microfluidic technologies are revolutionizing the way medicine and biology are approached. Ever smaller samples are being manipulated and analyzed more quickly and with greater accuracy than ever. As these performance metrics

C. Floryan
School of Engineering and Applied Sciences, Harvard University, Cambridge, MA, USA

D. Issadore
Bioengineering, University of Pennsylvania, Philadelphia, PA, USA
e-mail: Issadore@seas.upenn.edu

R.M. Westervelt (✉)
School of Engineering and Applied Sciences, Harvard University, Cambridge, MA, USA

Department of Physics, Harvard University, Cambridge, MA, USA
e-mail: westervelt@seas.harvard.edu

improve, new microfluidic applications in enzymatic assays, genomics, proteomics, and clinical pathology are becoming feasible [1–5].

Combining microfluidics with the power of electronics is a recent and growing trend empowering many new biological and medical applications. Microelectronics offer new and exciting ways to position and analyze cells and fluids [6–9]. They enable tremendous miniaturization, greater accuracy, discrete sample handling, and the ability to perform hundreds or even thousands of functions in parallel.

Integrated circuits (ICs) have the ability to empower even further miniaturization and complexity of biomanipulation and analysis devices. Integrated circuits combine the power of programmability with CMOS technology to fit billions of transistors on a single chip. Hybrid integrated circuits/microfluidic chips are capable of performing intricate manipulations and analysis on single cells and small chemical volumes [5, 10–17]. These devices pave the way for a new generation of miniaturized biomedical experiments which can be performed on single drops of human physiological fluids to diagnose illness and disease in a point-of-care setting.

Currently, the analysis of human physiological fluids is an often unpleasant and slow process. A large and painful syringe is first used to collect blood samples, after which the sample must be sent to a laboratory for analysis, delaying the results by days [18]. The vision driving integrated circuits/microfluidic technology is to take hundreds of existing tests and perform them quickly and simultaneously using a single nanoliter droplet of body fluid. The tests will be completed at the patient's bedside and, in minutes, empowering doctors with real-time knowledge of the patient's condition. The tests can also be performed in resource-limited settings such as developing countries, remote locations, and war zones.

Figure 2.1 shows an illustration of a hybrid integrated circuit/microfluidic chip for point-of-care diagnostics. Cells and reagents enter the device through inlets. Single cells and droplets are pinched off into the microfluidic chamber. The integrated circuit then positions the cells and droplets using electric fields. Sensors built into the integrated circuit analyze various properties of the cells and droplets and monitor the outcomes of chemical reactions.

Numerous new technologies and methods are needed to make integrated circuits for point-of-care diagnostics a reality. Many have already been developed and many more are in the pipeline. This chapter presents an overview of the current state of the field and a vision of future work needed to make ICs a reality in point-of-care diagnostics. Table 2.1 below summarizes functions which can be performed and on IC/microfluidic chips.

2.2 Principles of Dielectrophoresis

Most functions listed in the summary table above make use of electrical phenomena to manipulate and analyze droplets and cells. *Dielectrophoresis* is the bedrock phenomenon used to transport droplets. *Electroporation* and *dielectric heating* are

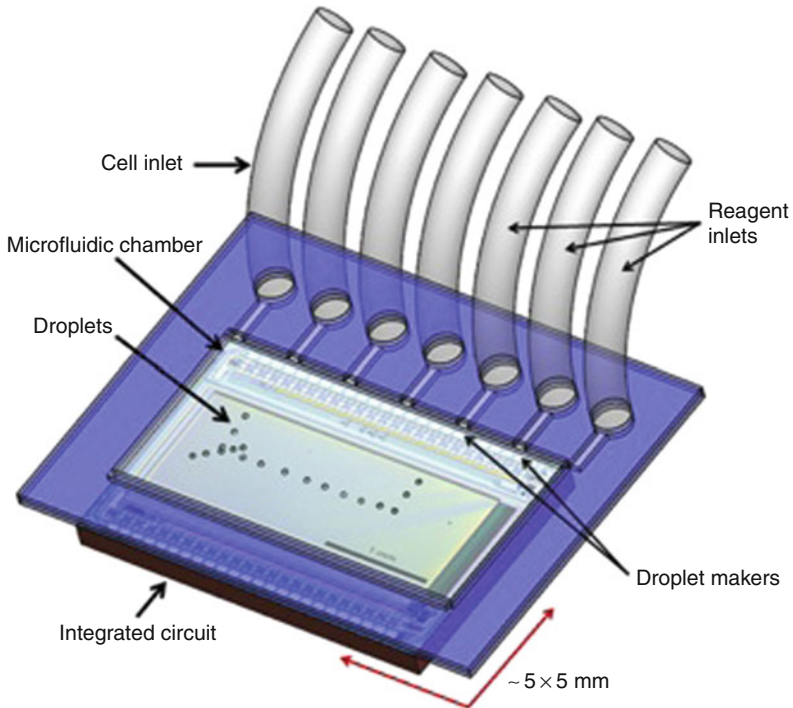







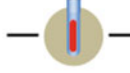
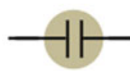



Fig. 2.1 An illustration of a hybrid integrated circuit/microfluidic chip for point-of-care diagnostics. The device contains an integrated circuit with a microfluidic chamber built on top. Cells and reagents enter through the inlets. Single cells and droplets are pinched off into the microfluidic chamber where they are positioned and analyzed

used to release cell contents, merge droplets, and heat the chip. All make use of alternating electric fields in different frequency bandwidths.

Dielectrophoresis (DEP) is a phenomenon where dielectric objects are attracted to electric field maxima. The object's polarizability relative to the surrounding medium determines the strength of DEP. It comes in two flavors, positive DEP and negative DEP, as seen in Fig. 2.2. With positive DEP, a dielectric particle is *more* polarizable than the surrounding medium and is attracted to the electric field *maxima*. This is shown with the upper particle of Fig. 2.2. In negative DEP, seen at the bottom of Fig. 2.2, the particle is *less* polarizable than the surrounding medium and is pushed away from the electric field maximum. This is analogous to a helium-filled balloon. Even though gravity is pulling it down, it floats upward because it is less dense than the surrounding air.

The force generated by dielectrophoresis is described by the following equations [19]:

Table 2.1 Functions performed on integrated circuits for medical diagnostics

	Function	Description	Diagram
1	Transport / Programmable Channels	Droplets of physiological fluids, reagents, and cells are moved using dielectrophoresis and magnetophoresis	
2	Deform	Electric and fields deform droplets by pulling them from different directions.	
3	Porate	Controllable mixing between the interior and exterior of cells and droplets	
4	Merge	Cells and droplets are merged with reagents to initiate chemical reactions.	
5	Temperature Control	Droplets and cells are heated by applying a microwave frequency electric field (1-3GHz).	
6	Temperature Sensor	Temperature is monitored to initiate or terminate temperature-dependent reactions.	
7	Capacitance Sensor	Capacitance measurements monitor electrical properties of cells and droplets.	
8	Droplet Maker	Droplets of external fluid are dispensed onto the chip using a droplet maker.	
9	Mix	Mixing to initiate chemical reactions	
10	Imaging	Fluorescence and color detection monitors reaction outcomes.	

$$F_{DEP} = 2\pi \epsilon_m r^3 CM(\omega) \nabla E_{RMS}^2 \quad (2.1)$$

$$CM(\omega) = Re \left(\frac{c_p - c_m}{c_p + 2c_m} \right) \quad (2.2)$$

where F_{DEP} is the dielectrophoretic force, ϵ_m is the permittivity of the surrounding medium, r is the particle's radius, CM is the Clausius–Mossotti factor, E is the

Fig. 2.2 An illustration of positive and negative dielectrophoresis (DEP). The *top* object is undergoing *positive* DEP, being pulled *toward* the electric field maxima. Its dielectric constant is greater than that of the surrounding medium. The *bottom* object is being pushed *away* from the maximum by *negative* DEP. Its dielectric constant is less than that of the surrounding medium

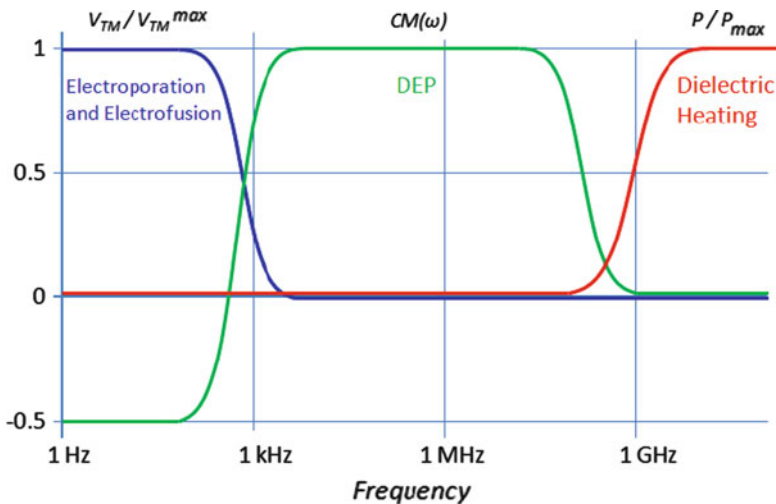
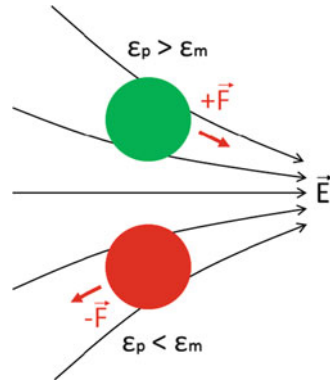


Fig. 2.3 A plot of three frequency regimes for vesicles. In the 1-Hz–1-kHz range, electroporation and electrofusion dominate. In the 1-kHz–10-MHz range, dielectrophoresis (*DEP*) dominates. Above 1 GHz, microwave heating dominates [10]

electric field, and ϵ_p is the particle’s permittivity. The strength and sign up the DEP force depends heavily on the frequency of the electric field, which is embedded in the complex permittivities in the Clausius–Mossotti factor. DEP for cells floating in water is optimal at a frequency of approximately 1 MHz. This is illustrated in Fig. 2.3 with the curve labeled “DEP.”

As shown in Fig. 2.3, different functions can be performed on cells and vesicles at various electric field frequencies. At low frequencies, cells can be porated and fused. The 1-Hz–1-kHz range destabilizes vesicles by creating a potential across their membranes. A large enough potential causes dielectric breakdown of the

membrane. At higher frequencies in the 1-kHz–10-MHz range, DEP dominates over electroporation and electrofusion. The electric field is switching faster than the vesicle membrane’s time constant, preventing voltage from building up across it. At even higher frequencies in the 1-GHz range, microwave heating becomes dominant.

2.3 Integrated Circuit/Microfluidic Chips

Integrated circuit/microfluidic chips contain displays of electrical pixels which are used to trap and position thousands of cells and droplets. Activating a pixel produces an electric field which dielectrophoretically attracts and traps cells. By simultaneously activating thousands of pixels, large numbers of cells can be precisely trapped and positioned.

Integrated circuit/microfluidic chips have undergone an evolution in the past decade, progressively increasing in complexity and incorporating more functions. Table 2.2 details the evolution of these chips – beginning with built-in-house DEP chips containing only 25 pixels and leading to present CMOS devices capable of producing both electric and magnetic fields and containing up to 32,000 pixels.

The second generation of hybrid IC/microfluidic chips shown in Table 2.3 uses CMOS integrated circuit technology. The chip is shown in Fig. 2.4 and consists of a display of 128×256 electrical pixels [14]. Each pixel is individually addressable and contains a single SRAM memory element. The inset in Fig. 2.3 shows two active pixels radiating electric fields and polarizing and trapping a nearby dielectric particle. Multiple pixels can be activated simultaneously. The pixels are $11 \times 11 \mu\text{m}^2$ in area, about the size of a living cell, and the entire chip is $2.3 \times 3.3 \text{ mm}^2$. The pixels are covered in a $2\text{-}\mu\text{m}$ thick layer of polyamide insulator to prevent short circuiting.

Active pixels are charged by an AC square wave running between 0 and 5 V. The frequency is set between 1 Hz and 1.8 MHz. Inactive pixels are also connected to an AC square wave, but are run out of phase with the active pixels. This creates electric field maxima at the *interface* between active and inactive pixels – this is where cells are trapped by DEP.

The third-generation chip, shown in Fig. 2.5, incorporates larger voltages and the ability to generate magnetic fields [6]. Larger voltages generate stronger DEP forces which position cells faster and more reliably. Higher voltages also allow cells to be electroporated which enables cell fusion and the transport of foreign particles across the cell membrane. Magnetic fields are generated to enable functionalized magnetic particles – often used in the biomedical community – to be used with this chip.

This chip is a CMOS integrated circuit with an array of 60×61 electric pixels, as seen in Fig. 2.5b. Each pixel is individually addressable and can be activated to 0 or 50 V. Similar to the second-generation chips, pixels are activated by sending an AC electrical signal. Inactive pixels are run out of phase, creating electric field maxima at the interface between active and inactive pixels. This is where cells are trapped by DEP. This chip can also generate magnetic fields using a 60×60 array of

Table 2.2 Progression of integrated circuit/microfluidic chips




Chip	Field	Number of pixels	Technology	Picture
DEP Chip 1st generation [15]	Electric	5 x 5	Built in-house	
2nd generation [14]	Electric	128 x 256	CMOS	
3rd generation [11]	Electric and Magnetic	60 x 61 electric 60 x 60 magnetic	CMOS	

Table 2.3 Characteristics of the second-generation DEP chip

Process	MOSIS TSMC 0.35 μm gate length 2PM4 process
Pixel size	$11 \times 11 \mu\text{m}$
Pixels	128×256
Chip size	$2.3 \times 3.3 \text{ mm}^2$
Addressing	8-bit word line decoder, 128-bit, two-phase clocked shift register for bit lines
Transistor count	$>360,000$
Pixel voltage	$V = 3\text{-}5 \text{ V}$, DC – 1.8 MHz
Operating current	30–100 mA

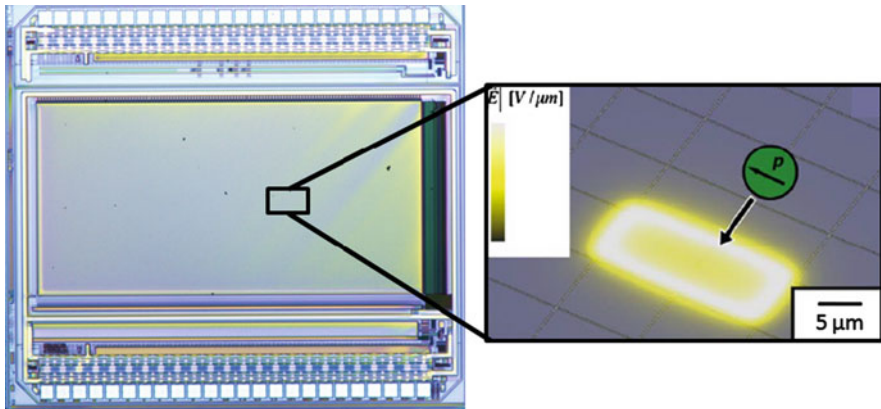


Fig. 2.4 The second generation of hybrid IC/microfluidic chip incorporates a CMOS integrated circuit. This chip contains a display of 128×256 pixels, each individually addressable and $11 \times 11 \mu\text{m}^2$ in area. The entire chip is $2.3 \times 3.3 \text{ mm}^2$ large. The *inset* shows two active pixels producing electric fields and attracting a nearby dielectric particle

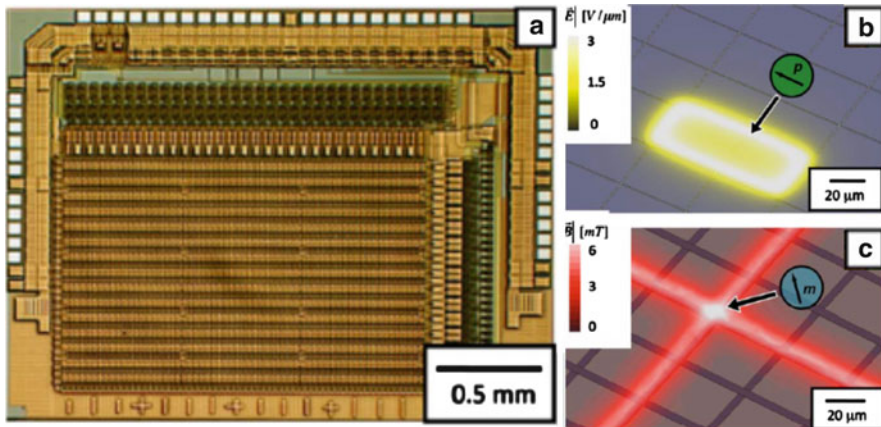


Fig. 2.5 (a) The third-generation chip consists of an array of 60×61 pixels and 60×60 wires. (b) The pixels are charged to 0 or 50 V to generate electric fields. (c) The wires carry current to generate magnetic fields. Magnetic field maxima occur where two orthogonal wires overlap

wires, shown in Fig. 2.5b. The wires are activated by running a 120-mA DC current through them. Magnetic field maxima are generated where two perpendicular wires overlap, creating a trap for magnetic particles [13].

2.4 Functions Performed by Hybrid Integrated Circuit/Microfluidic Chips

Many functions have been implemented on integrated circuits for medical diagnostics. Droplets and cells can be transported, deformed, porated, merged, and heated [10–15]. Virtual microfluidic channels, defined by electric field boundaries, have also been implemented. Temperature and conductance sensors have also been built into IC's [14, 17]. These functionalities are described in further detail in the remainder of this chapter. Several important operations have also yet to be implemented on an integrated circuit platform for diagnostics. These include droplet making, mixing, and color and fluorescence sensing. These will round off the remainder of this chapter.

2.4.1 Positioning/Programmable Channels

Positioning cells and droplets, shown in Fig. 2.6, is a critical function underpinning the usefulness of integrated circuit technology for medical diagnostics. Reagents must be transported from storage areas onto the chip and mixed and reacted with

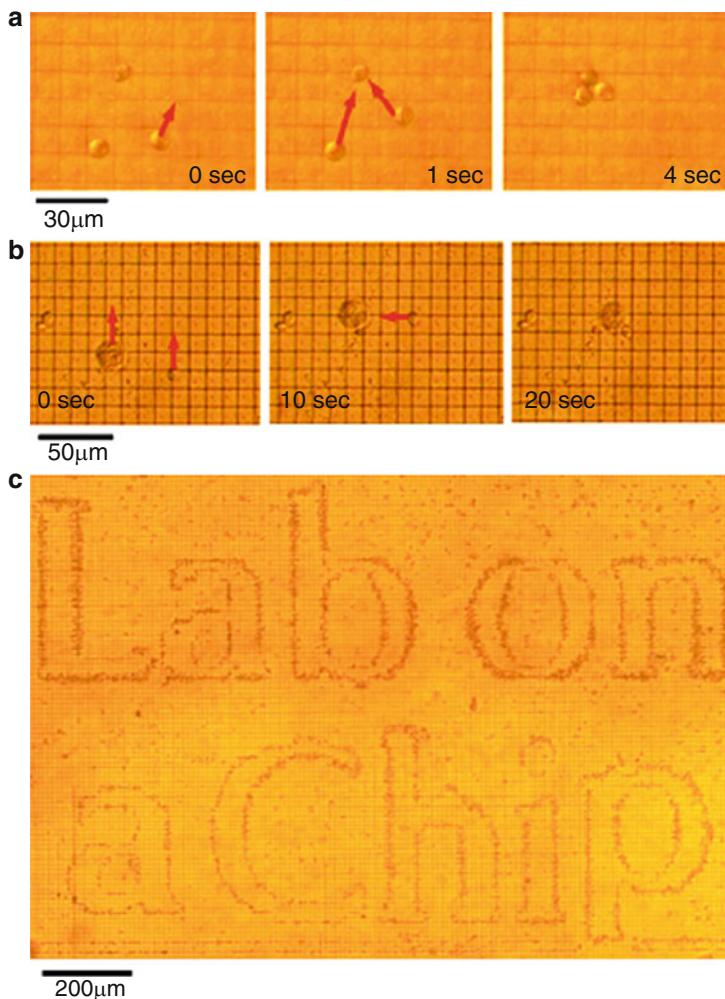


Fig. 2.6 (a) Two cells are positioned using the integrated circuit's pixel display. (b) A rat macrophage and a yeast cell are positioned. (c) Yeast cells are arranged into a complex pattern spelling out "Lab on a Chip," the title of the journal where this work was first published

blood, urine, cells, and other human samples. The resulting reactants are positioned over sensing regions of the chip for analysis. The positioning process must be capable of multiplexing hundreds of droplets simultaneously and without collisions to allow multiple diagnostic tests to be performed in parallel.

Figure 2.6 shows cells and droplets being trapped and positioned using a hybrid integrated circuit/microfluidic chip. A cell is trapped over an active pixel and positioned by shifting the pixel's voltage onto neighboring pixels [14]. Cells and droplets follow the electric field maximum as it moves from pixel to pixel. Figure 2.6

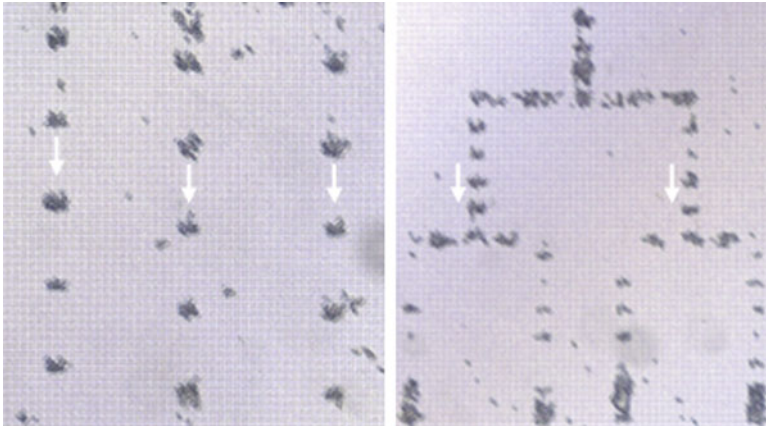


Fig. 2.7 Virtual microfluidic channels are created using trains of moving pixels. Every tenth pixel in a line is active, with each one transporting several cells. Linear channels can also be combined with junctions to create the branching configurations seen on the *right*

shows (a) two similar cells being moved by the second-generation integrated circuit and (b) two different strains of cells moving over the integrated circuit. An active pixel potentiated to 5 V creates approximately 5 pN of force on a cell, transporting it at up to 300 $\mu\text{m/s}$. The cells are exposed to electric fields of up to 50 kV/m at 1 MHz, well within the range where they remain healthy. Thousands of cells were also positioned simultaneously to form a complex and well-defined structure, as seen in Fig. 2.6c. The phrase “lab on a chip” is spelled using yeast cells.

Virtual microfluidic channels were created using the hybrid integrated circuit/microfluidic chip. Figure 2.7 shows two such arrangements where three channels are run in parallel and where one channel is branched into four. Cells are carried by trains of pixels where active pixels are separated by several inactive pixels. In Fig. 2.7, every tenth pixel was active. The active pixels each move in the same direction and each one carries several cells. Virtual microfluidic channels are created similarly to videos on the chip. A video file contains a number of frames where a train of pixels moves one position with each subsequent frame. Each video encodes a different configuration of channels, allowing a single chip to perform many tasks simply by playing a different video.

Thousands of cells can also be moved simultaneously on the chip. Figure 2.8 shows frames from a video where thousands of yeast cells were positioned to move like a dancer. The dancer is approximately 1.5 mm tall. Active pixels are located inside the dancer, drawing cells to the edge of the dancer where the electric field is strongest. This video was created by sending a GIF video file to the chip. A new frame is displayed on the chip several times every second, moving the cells as each new frame is displayed. Figure 2.8 shows frames 5 s apart with one additional frame inserted at 0:17 s to show the dancer’s full range of motion.

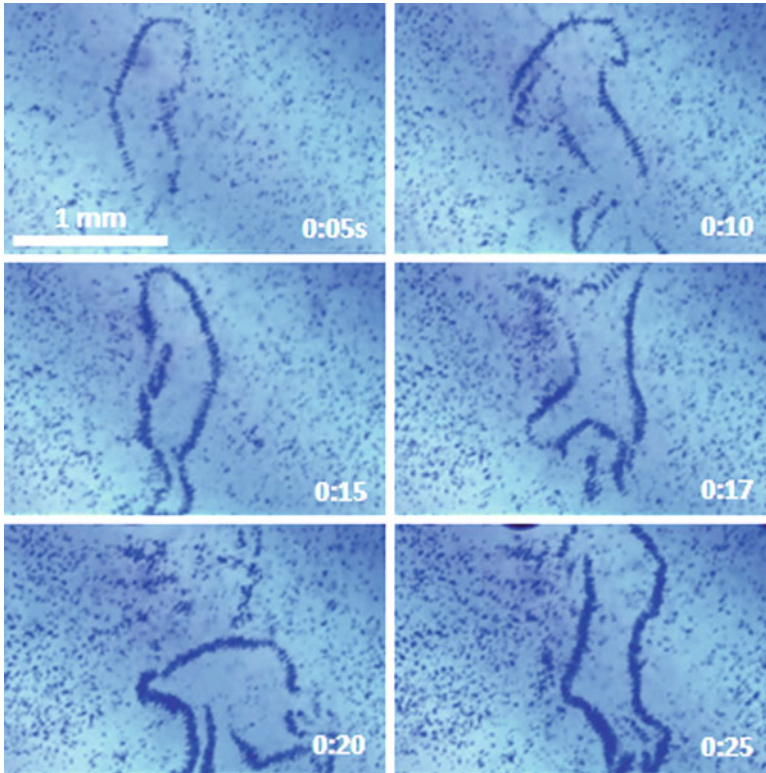


Fig. 2.8 A video is played on the chip where thousands of yeast cells are moved in the shape of a dancer. The video is sent to the chip as a GIF file

2.4.2 Deform

The chip can be used to deform vesicles into different shapes, shown in Fig. 2.9 [10]. This has important implications for single-vesicle and single-cell rheology where microscopic control is essential for studying these complex systems. It represents an alternative to microcontact patterning [20] and other existing methods for single-cell studies. Figure 2.9 shows vesicles being stretched, compressed, and being deformed into various shapes with flat edges. The first column in the figure shows the active pixels shaded. The second column shows the results of electric field simulations mapping the field amplitude where brighter red colors represent stronger fields. The third column shows images of vesicles being deformed. The vesicles are approximately $50\ \mu\text{m}$ in diameter and can be stretched, compressed, and deformed into squares, diamond, and hexagons.

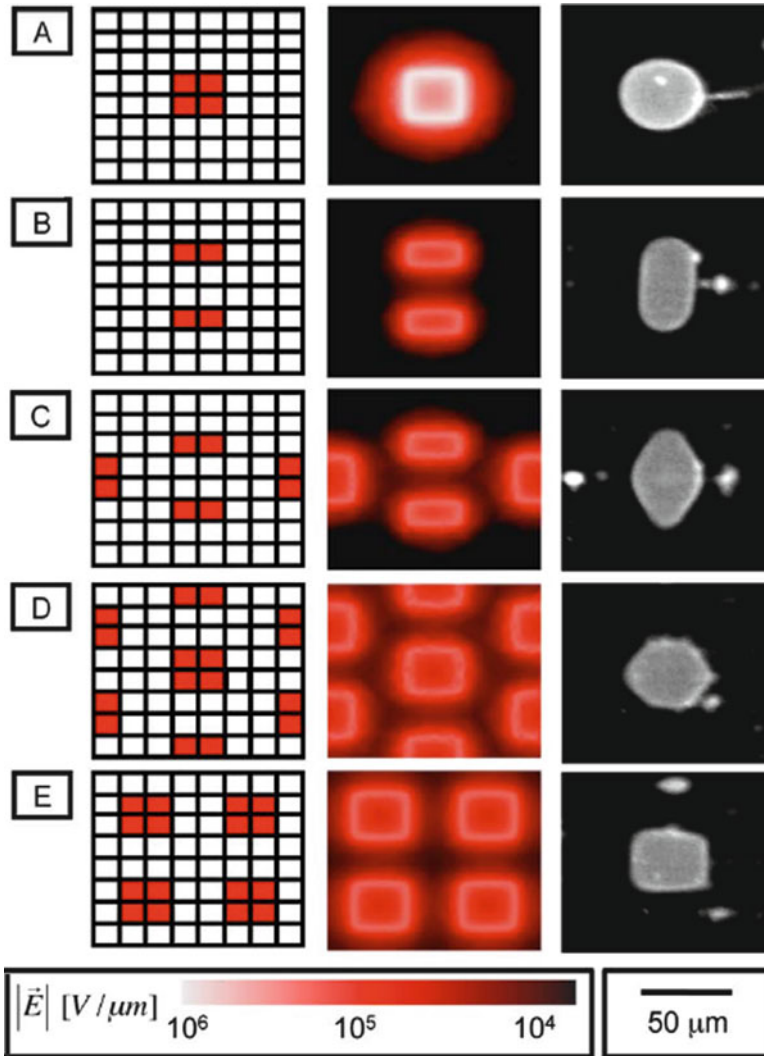


Fig. 2.9 Vesicles are deformed into several different shapes by activating different combinations of pixels

The hybrid integrated circuit/microfluidic chip is used to deform a vesicle containing magnetic particles, shown in Fig. 2.10 [10, 11]. The chip combines both an array of electric pixels and an array of magnetic wires. The vesicle is first trapped dielectrophoretically by activating the pixels below it, while a magnetic field traps the iron oxide particle. The magnetic field maximum is moved away from the vesicle, dragging the magnetic particle and elongating the vesicle. Once

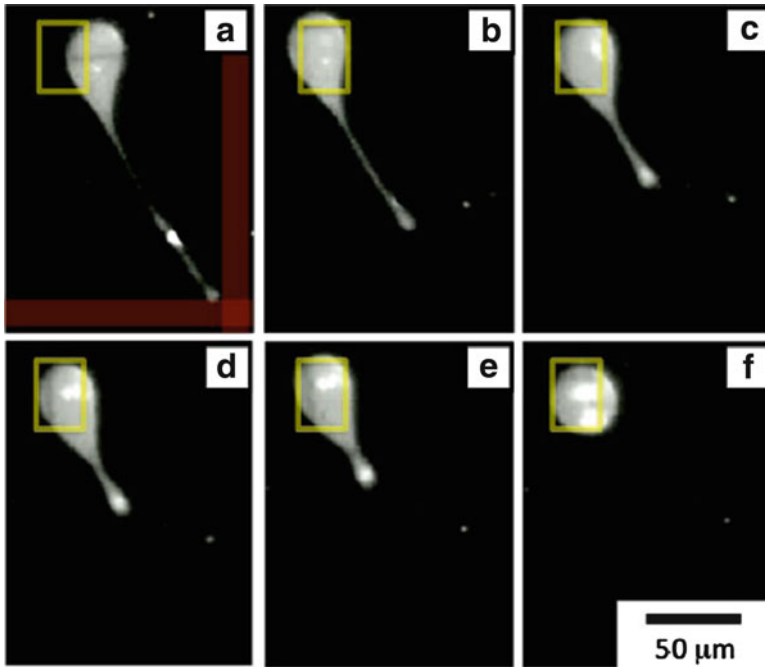


Fig. 2.10 A combination DEP/magnetic chip deforms a vesicle. The vesicle is held in place by dielectrophoresis while a magnetic field pulls an iron oxide particle out of the vesicle

the magnetic field is turned off, the vesicle contracts back to its original shape. This chip can be useful in single-cell rheological studies for point-of-care diagnostics.

2.4.3 Porate

Poration is used to release vesicle contents, as seen in Fig. 2.11. Electroporation involves using electric fields to destabilize the vesicle membrane and create small, short-lived holes [21]. The holes are large enough to allow macromolecules to enter and leave the vesicle. AC electric fields in the 1-Hz–10-kHz range induce transmembrane voltages large enough to cause a dielectric breakdown of the membrane, thus destabilizing it [21, 22]. In Fig. 2.11, a vesicle was placed in a fluid containing fluorescein, a fluorescent molecule [10, 12]. At time $t = 0$ s, the vesicle was electroporated, allowing fluorescein to enter. In a second experiment, a vesicle was prefilled with fluorescein and submerged in water. It was similarly electroporated, diffusing away its fluorescein and losing its fluorescence.

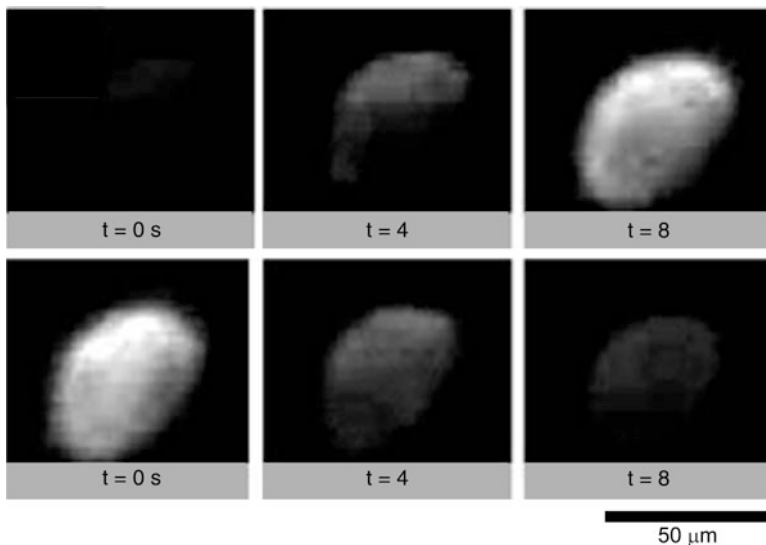
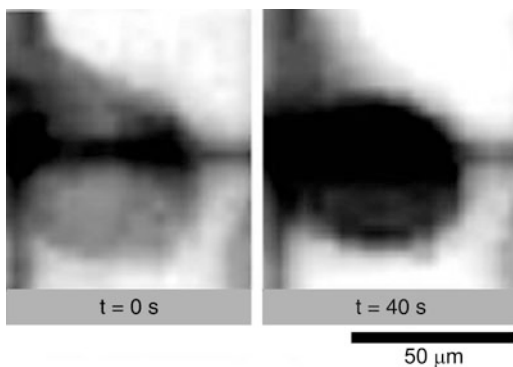


Fig. 2.11 Vesicles were electroperated using a hybrid integrated circuit/microfluidic device. At $t = 0$ s in the *upper left corner*, a vesicle surrounded by fluid containing fluorescein, a fluorescent molecule, was electroperated. The molecule entered the vesicle, making it fluoresce at $t = 8$ s. At time $t = 0$ s in the *lower right corner*, a fluorescent vesicle was electroperated. The fluorescein diffused into the surrounding fluid

Fig. 2.12 A cell is electroperated using the hybrid integrated circuit/microfluidic chip. The cell membrane is normally impermeable to trypan blue, a dye commonly used to stain cells, but after electroperation, it enters and darkens the cell



Cells can also be electroperated to insert contents into the cell and to release its contents, as seen in Fig. 2.12. This is a critical function enabling biological vectors and functionalized particles to be introduced into the cell and to analyze the cell contents [22–24]. Cell electroperation is demonstrated by placing a yeast cell on the hybrid integrated circuit/microfluidic chip in a solution containing trypan blue, a dye commonly used for staining biological samples [10, 12]. The cell membrane is impermeable to trypan blue. The cell was trapped above a

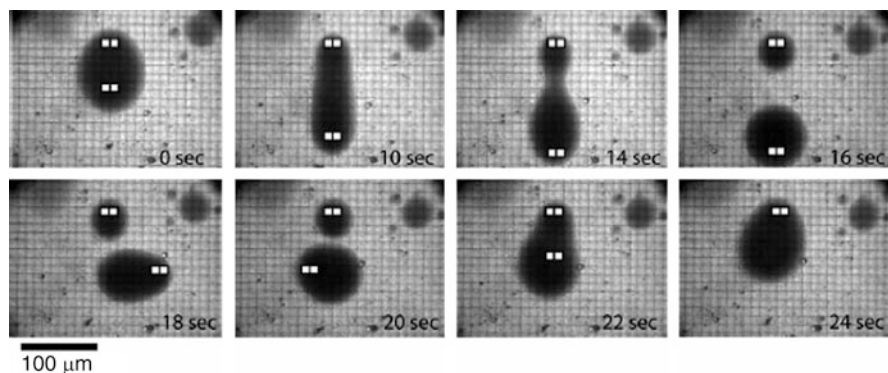


Fig. 2.13 The hybrid integrated circuit/microfluidic chip splits a droplet and subsequently merges it. The droplets are composed of oil submerged in a water medium

pixel using DEP, after which the electric field was switched to a lower frequency, triggering electroporation. After 40 s, the trypan blue had entered and stained the cell, confirming that electroporation had indeed occurred.

2.4.4 Merge

Figures 2.13 and 2.14 demonstrate how a simple fluid droplet can be split into two, with one individually manipulated, and then rejoined into one. Merging droplets is an essential function for performing chemical reactions on the chip. A sample and multiple reagents are each contained in individual droplets. The reaction is instigated by merging the droplets together, bringing the different reagents into contact with the sample. Droplet merging is performed by moving the active pixels under each droplet together, as seen in Fig. 2.13 [10, 12]. When the two neighboring droplets come into contact, they merge into a single, larger drop. After completion of a reaction, the analytes are transported to an area of the chip with sensing capabilities.

Cell fusion is a critical technique enabling cellular reprogramming, cloning, and hybridoma formation [25–31]. A method for fusing cells using a hybrid integrated circuit/microfluidic chip was developed and is shown in Fig. 2.15. The chip traps and moves cells using dielectrophoresis, positioning the cells into pairs in preparation for cellular fusion. Fusion was performed using electroporation or by introducing PEG (polyethylene glycol) into the system. Our technique has the advantage of precise control over every cell, allowing perfect pairing of cells every time and thus significantly increasing the yield. Fusion was performed in three different configurations: An individual pair of cells was isolated and fused, several pairs of cells were isolated and fused, and thousands of cell pairs were fused simultaneously.

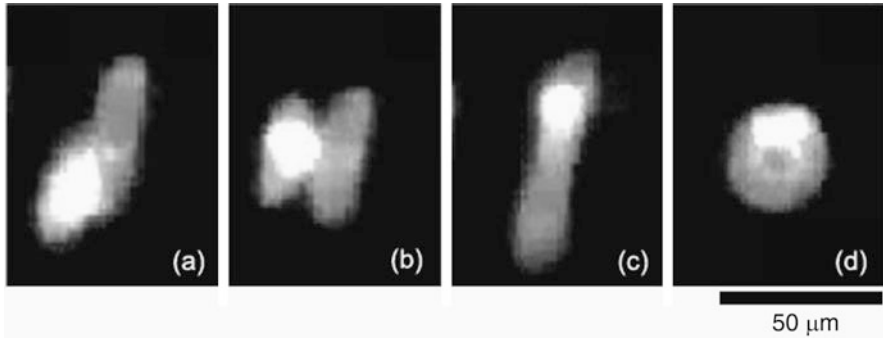


Fig. 2.14 The hybrid integrated circuit/microfluidic chip fuses two vesicles

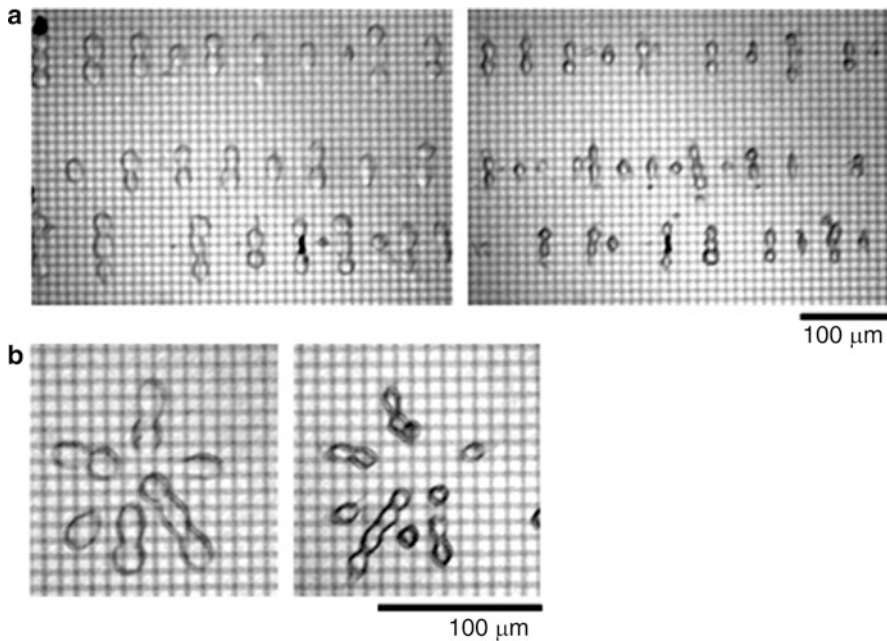


Fig. 2.15 Cell fusion was performed on the integrated circuit/microfluidic chip. Dielectrophoresis was used to arrange the cells in different configurations (**a**, **b**), and electrofusion and chemical fusion were used to merge neighboring cells

Cells were fused both stochastically and deterministically—stochastic pairing results in random cells being fused together, while deterministic pairing ensures that *each* pair contains one cell from both cell lines. Viable fused cells with a mean yield of 89% were observed. Figure 2.15a shows multiple pairs of cells being aligned in rows and fused, and Fig. 2.15b shows cells being arranged in a circle for fusion.

2.4.5 Temperature Sensor

Temperature sensors are an important component for integrated circuits to become viable in medical diagnostics. Cells must often be viable for extended periods of time, requiring on-chip incubation and temperature monitoring. Analytes and physiological fluids must frequently be maintained at specific temperatures for proper chemical activation. Biochemical reactions are also often initiated and terminated by temperature changes—a well-known example being polymerase chain reaction (PCR). To this end, recent IC/microfluidic chips have had multiple temperature sensors integrated into their architecture, allowing the temperature to be monitored independently over different regions of the chip [12]. They consist of micron-scale thermistors built under the IC surface. They work by monitoring temperature-dependent resistance changes and calibrating them to a temperature scale. A feedback loop with an external cooling apparatus then maintains the chip at the desired temperature.

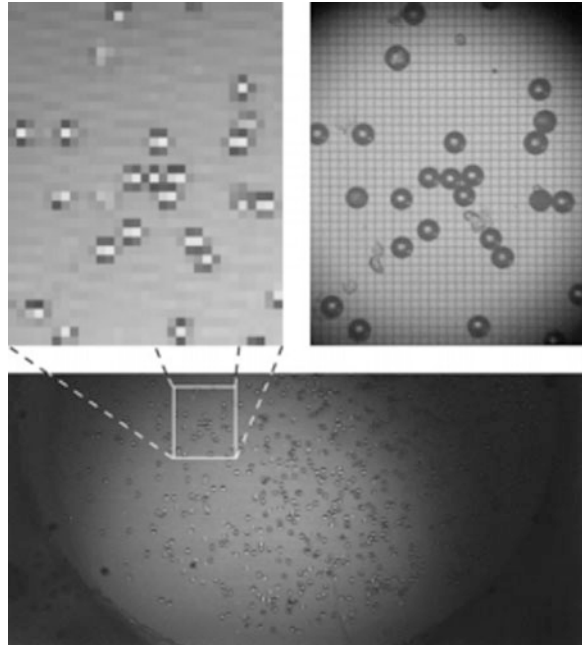
2.4.6 Microwave Dielectric Heating

Microwave dielectric heating has been developed for warming small, micron-sized droplets in oil [32]. Electric fields in the 1–3-GHz bandwidth – in the microwave spectrum – are transmitted across droplets, causing rapid and well controlled heating of the droplets without heating the surrounding environment directly. The advantage of heating such small-length scales is the high surface-to-volume ratio, allowing rapid thermal cycling in the 15-ms range. The technology is scalable onto an integrated circuit platform, with each individual pixel acting as a microwave heater. This enables the highly localized heating and incubation of droplets and cells.

2.4.7 Capacitance Sensor

Sensing the capacitive coupling between a pixel and an object on top can be used to inform the device where droplets and cells are located. This is seen in Fig. 2.16. This is critical for giving the chip feedback capabilities and is a method for error checking that a cell or droplet indeed moved to the position it was instructed. Capacitive sensing can eliminate the need for the hybrid integrated circuit/microfluidic chip to be placed under an optical microscope. In Fig. 2.16, capacitive sensors were embedded under every pixel, giving high-resolution images of cells and beads resting on the chip's surface [17]. The sensors discerned differences in electrical properties in the medium directly above the chip, and mapped them as grayscale images. Fig. 2.16 shows the image obtained from the chip's embedded sensors next to an image of the same region taken with an optical microscope.

Fig. 2.16 Built-in sensors in the chip are capable of creating images by mapping electrical properties of the medium in contact with the chip's surface. On the *left-hand side* is an image of beads created using this method. On the *right-hand side* is the same image taken with an optical microscope [17]



2.4.8 *Integrating Hybrid IC/Microfluidic Chips with Other Technologies*

Hybrid integrated circuit/microfluidic chips can be integrated with other technologies to increase their ability to solve problems in point-of-care diagnostics. Improved methods for intaking fluids – blood, urine, and chemical reagents – from the outside environment are critical for the success of hybrid IC/microfluidic chips. Methods to mix very small volumes of fluid are also necessary to allow reagents to properly and fully mix with the analytes. This is a difficult problem at small-size scales, and inspiration can be borrowed from electrowetting and magneto-mechanical mixing techniques.

There is a strong need for more automated and sophisticated methods of pulling fluids directly out of the environment and dispensing them as droplets on the hybrid IC/microfluidic chip. This functionality promises to make the chip more self-contained and independent, eliminating the need for technicians and external syringe pumps to deliver fluids. Electrical methods of pulling droplets from fluid reservoirs have previously been demonstrated. Electrowetting is one commonly cited method [33, 46], using electrically induced differences in the wettability of adjacent surfaces to move and split droplets [39].

Mixing is an important function in microfluidic devices, significantly accelerating the rate and accuracy of biochemical reactions. Small fluid volumes are

especially difficult to mix as they have a tendency to remain in the laminar flow regime. In this regime, flow-vector lines do not intersect, and mixing remains slow. Several methods have been demonstrated to overcome this challenge for droplets in the millimeter-size range. Such droplets were rapidly actuated between neighboring pixels using electrowetting, inducing internal flow fields [37]. Dielectrophoresis-induced flows can also be used. Another approach uses magneto-mechanical mixing [47]. Superparamagnetic beads were inserted into unilamellar vesicles, and an external magnetic field was applied, aligning the beads into chains. As the magnetic field rotated, the vesicle contents were mixed by the spinning chains. The vesicles were 10–20 μm in diameter – the same size-scale as droplets and cells used in hybrid IC/microfluidic chips.

2.5 Conclusions

This chapter describes the development of a versatile platform for point-of-care diagnostics using integrated circuit (IC) technology. This work is an important step toward developing automated, portable, and inexpensive devices to perform complex chemical and biological tasks. Such a device would revolutionize the way that biological and chemical information is collected for medical diagnostics, allowing doctors to make near real-time prognoses.

The hybrid IC/microfluidic chips developed thus far control living cells and small volumes of fluid. Table 2.1 summarized the basic lab-on-a-chip functions that the hybrid chips can perform. The chips can be programmed to transport, deform, porate, and merge droplets and cells; they can control temperature, sense temperature, sense capacitance, and sense color and fluorescence, and they can make and mix droplets. These basic functions can be strung together to perform complex chemical and biological tasks. The fast electronics and complex circuitry of ICs enable thousands of living cells and droplets to be simultaneously controlled, allowing many well-controlled biological and chemical operations to be performed in parallel. With ICs becoming more powerful each year and microfluidics beginning to enter the commercial arena, IC/microfluidic chips are poised to play an important role in clinical diagnostics.

References

1. T.M. Squires, S.R. Quake, Microfluidics: Fluid physics at the nanoliter scale, *Rev. Mod. Phys.* vol. **77**, pp. 977–1026, (2005)
2. D.J. Beebe, G.A. Mensing and G.M. Walker, Physics and applications of microfluidics in biology, *Annu. Rev. of Biomedical Eng.* **4**, 261–286, (2002)
3. C. Hansen and S.R. Quake, Microfluidics in structural biology: smaller, faster ... better, *Current Opinions in Structural Biol.* **13**(5), 538–544 (2003)

4. D.B. Weibel, G.M. Whitesides, Applications of microfluidics in chemical biology. *Curr. Opin. Chem Biol.* **10**, 584–591 (2006)
5. G.M. Whitesides, The origins and the future of microfluidics. *Nature*, **442**, 368–373 (2006)
6. H. Lee, D. Ham, R.M. Westervelt (eds.) *CMOS Biotechnology (Integrated Circuits and Systems)*, (Springer, New York, 2007)
7. S.K. Sia, L.J. Kricka, Microfluidics and point-of-care testing, *Lab Chip*, **8**, 1982–1983 (2008)
8. A. Wu, L. Wang, E. Jensen, R. Mathies, B. Boser, Modular integration of electronics and microfluidic systems using flexible printed circuit boards. *Lab Chip* **10**, 519–521, (2010)
9. P. Pittet, L. Guo-Neng, J.-M. Galvan, R. Ferrigno, L.J. Blum, B.D. Leca-Bouvier, PCB technology-based electrochemiluminescence microfluidic device for low-cost portable analytical systems. *Sensors J. IEEE* **8**, 565–571 (2008)
10. D. Issadore, T. Franke, K.A. Brown, R.M. Westervelt, A microfluidic microprocessor: controlling biomimetic containers and cells using hybrid integrated circuit/microfluidic chips. *Lab Chip*, **10**, 2937–2943 (2010)
11. D. Issadore, T. Franke, K.A. Brown, T.P. Hunt, R.M. Westervelt, High voltage dielectrophoretic and magnetophoretic hybrid integrated circuit/microfluidic chip. *IEEE J. Microelectromech. Syst.* **18**, 1220 (2009)
12. D. Issadore, Hybrid integrated circuit/microfluidic chips for the control of living cells and ultra-small biomimetic containers, Ph.D. Thesis. Harvard University, Cambridge, MA, 2009 (Print)
13. H. Lee, Y. Liu, D. Ham, R.M. Westervelt, Integrated cell manipulation system—CMOS/microfluidic hybrid. *Lab Chip* **7**, 331–337, (2007)
14. T.P. Hunt, D. Issadore R.M. Westervelt, Integrated circuit/microfluidic chip to programmably trap and move cells and droplets with dielectrophoresis. *Lab Chip*, **8**, 81–87, (2007)
15. T.P. Hunt, H. Lee, R.M. Westervelt, Addressable micropost array for the dielectrophoretic manipulation of particles in fluid. *Appl Phys. Lett.* **85**, 6421 (2004)
16. P.R. Gascoyne, J.V. Vykoukal, J.A. Schwartz, T.J. Anderson, D.M. Vykoukal, K.W. Current, C. McConaghy, F.F. Becker, C. Andrews, Dielectrophoresis-based programmable fluidic processors. *Lab Chip* **4**, 299–309 (2004)
17. N. Manaresi, A. Romani, G. Medoro, L. Altomare, A. Leonardi, M. Tartagni, R. Guerrieri, A CMOS chip for individual cell manipulation and detection. *IEEE J. Solid-St. Circ.* **38**, 2297–2305, (2003)
18. Lab Tests Online, Collecting samples for testing (2011), <http://www.labtestsonline.org/understanding/features/samples.html>. Retrieved 17 May (2011)
19. T.B. Jones, *Electromechanics of Particles*, (Cambridge University Press, 1995)
20. M. Mrksich, L.E. Dike, J. Tien, D.E. Ingber, G.M. Whitesides, Using microcontact printing to pattern the attachment of mammalian cells to self-assembled monolayers of alkanethiolates on transparent films of gold and silver. *Exp. Cell Res.* **235**, 305–313 (1997)
21. U. Zimmermann, G. Pilwat, F. Riemann, Dielectric breakdown of cell membranes. *Biophysical J.* **14**(11), 881–899 (1974)
22. D. Change, Cell poration and cell fusion using an oscillating electric field. *Biophysical J.* **56**(4), 641–652 (1989)
23. H. Andersson, A. van den Berg, Microfluidic devices for cellomics: a review. *Sensors. Actuat. B Chem.* **92**, 315–325 (2003)
24. H. Lu, M.A. Schmidt, K.F. Jensen, A microfluidic electroporation device for cell lysis. *Lab Chip*, **5**, 23–29 (2005)
25. E.H. Chen (ed.), *Cell Fusion: Overview and Methods* (Humana Press, Totowa, 2010)
26. J.A. Nickoloff (ed.), *Animal cell electroporation and electrofusion protocols* (Humana Press, Totowa, 1995)
27. D.T. Chiu, A microfluidics platform for cell fusion. *Curr. Opin. Chem. Biol.* **5**, 609–612 (2001)
28. L. Olsson, H.S. Kaplan, Human-human hybridomas producing monoclonal antibodies of predefined antigenic specificity. *Proc. Natl. Acad. Sci. U.S.A.* **77**, 5429–5431 (1980)
29. K.H. Campbell, P. Loi, P.J. Otaogui, I. Wilmut, Cell cycle co-ordination in embryo cloning by nuclear transfer. *Rev. Reprod.* **1**, 40–46, (1996)

30. M. Lewitzky, S. Yamanaka, Reprogramming somatic cells towards pluripotency by defined factors. *Curr. Opin. Biotechnol.* **18**, 467–473 (2007)
31. T. Barberi, M. Bradbury, Z. Dincer, G. Panagiotakos, N.D. Socci, L. Studer, Derivation of engraftable skeletal myoblasts from human embryonic stem cells. *Nat. Med.* **13**, 642–648 (2007)
32. D. Issadore, K.J. Humphry, K.A. Brown, L. Sandberg, D. Weitz, R.M. Westervelt, Microwave dielectric heating of drops in microfluidic devices. *Lab Chip* **9**, 1701–1706, (2009)
33. M. Abdelgawad, A.R. Wheeler, The digital revolution: a new paradigm for microfluidics. *Adv. Mater.* **21**, 920–925 (2009)
34. R.B. Fair, A. Khlystov, T.D. Taylor, V. Ivanov, R.D. Evans, P.B. Griffin, V. Srinivasan, V.K. Pamula, M.G. Pollack, and J. Zhou, Chemical and biological applications of digital-microfluidic devices. *IEEE Des. Test of Comput.* **24**(1), 10 (2007)
35. A.R. Wheeler, Putting Electrowetting to Work. *Science.* **322**, 539–540 (2008)
36. V. Srinivasan, V.K. Pamula, and R.B. Fair, An integrated digital microfluidic lab-on-a-chip for clinical diagnostics on human physiological fluids. *Lab Chip* **4**, 310–315, (2004)
37. P. Paik, V.K. Pamula, and R.B. Fair, Rapid droplet mixer for digital microfluidic systems. *Lab Chip* **3**, 253–259, (2003)
38. Y.-H. Chang, G.-B. Lee, F.-C. Huang, Y.-Y. Chen, J.-L. Lin, Integrated polymerase chain reaction chips utilizing digital microfluidics. *Biomed. Microdevices* **8**, 215–225 (2006)
39. S.K. Cho, H. Moon, C.J. Kim, Creating, transporting, cutting, and merging liquid droplets by electrowetting-based actuation for digital microfluidic circuits. *J. Microelectromechanical syst.* **12**(1), 70 (2003)
40. F. Su, K. Chakrabarty, Architectural-level synthesis of digital microfluidics-based biochips, *Proceedings of the IEEE International Conference on CAD*, San Jose, California, USA, pp. 223–228, (2004)
41. A.R. Wheeler, H. Moon, C.J. Kim, J.A. Loo, and R.L. Garrell, Electrowetting-based microfluidics for analysis of peptides and proteins by matrix-assisted laser desorption/ionization mass spectroscopy. *Anal. Chem.* **76**, 4833–4838 (2004)
42. E.J. Griffith, S. Akella, M.K. Goldberg, Performance characterization of a reconfigurable planar-array digital microfluidic system. *IEEE Trans. Comput. Aided Des. Integr. Circuits Syst.* **25**, 345–357 (2006)
43. C.G. Cooney, C.Y. Chen, M.R. Emerling, A. Nadim, J.D. Sterling, Electrowetting droplet microfluidics on a single planar surface. *Microfluid Nanofluid.* **2**(5), 435–446 (2006)
44. J. Zeng, and T. Korsmeyer, Principles of droplet electrohydrodynamics for Lap-on-a-chip. *Lab Chip*, **4**, 265–277 (2004)
45. H. Yang, V.N. Luk, M. Abdelgawad, I. Barbulovic-Nad, A.R. Wheeler, A World-to-chip interface for digital microfluidics *Anal. Chem.* **81**, 1061–1067 (2009)
46. A.R. Wheeler, H. Moon, C.A. Bird, R.R. Ogorzalek Loo, C.J. Kim, J.A. Loo, R. L. Garrell, Digital microfluidics with in-line sample purification for proteomics analyses with MALDI-MS. *Anal. Chem.* **77**, 534–540 (2005)
47. T. Franke, L. Schmid, D.A. Weitz, A. Wixforth, Magneto-mechanical mixing and manipulation of picoliter volumes in vesicles. *Lab Chip* **9**, 2831–2835, (2009)